



Skin Disease Classification Using Hierarchical Convolutional Neural Networks

¹Harshitha Rai, ²Preksha C, ³Souksha H D, ⁴Vanya Kumari, ⁵Renita Pinto

¹Final Year B.E Student, ²Final Year B.E Student, ³Final Year B.E Student, ⁴Final Year B.E Student, ⁵Assistant Professor

¹Department of Information Science & Engineering,

¹Mangalore Institute of Technology & Engineering, Mangalore, India

Abstract: Dermatological disorders impact roughly one-third of humanity, creating substantial healthcare burdens through physical symptoms and emotional distress. Diagnosis timing presents critical obstacles stemming from inadequate specialist availability, expensive medical consultations, and prolonged scheduling delays. Our work introduces an artificial intelligence-driven analytical platform employing hierarchical convolutional architectures for automated pathological identification. This framework operates through dual-phase methodology: initial broad categorization followed by granular sub-classification refinement. Through exploiting pre-trained EfficientNetB3 architecture, our implementation demonstrates 81% primary-level precision across 3 broad categories (infectious, inflammatory, others) encompassing 23 disease classes and 62% secondary-level precision for fine-grained classification, achieving 71% overall accuracy after complete integration. The browser-based platform delivers instantaneous diagnostic assessments incorporating probability metrics and therapeutic guidance. Cloud-enabled model training through Google Colab facilitates efficient development eliminating specialized computing requirements, establishing an accessible screening mechanism particularly valuable for medically underserved communities.

Index Terms - Hierarchical CNN, Skin Disease Classification, Transfer Learning, Deep Learning, EfficientNetB3, Medical Image Analysis, Web-based Healthcare.

I. INTRODUCTION

Cutaneous pathologies represent significant global health challenges, impacting approximately thirty-three percent of worldwide populations while generating considerable discomfort alongside psychological burden. Prompt diagnostic assessment proves fundamental for therapeutic efficacy, yet multiple obstacles restrict timely intervention including critical physician shortages, prohibitive service expenses, extended consultation scheduling, and insufficient medical literacy especially throughout rural territories. Within emerging economies, specialist-to-patient proportions remain substantially inadequate relative to established guidelines, compelling individuals toward extensive travel for accessing specialized medical services.

Conventional diagnostic protocols encompassing tissue sampling, dermatoscopic examination, and allergen testing, despite demonstrating reliability, involve invasive procedures demanding substantial time investment and specialized instrumentation. Visual evaluation maintains inherent subjectivity correlating with practitioner experience potentially yielding inconsistent diagnostic conclusions. Contemporary developments within artificial intelligence and machine learning frameworks present promising alternatives. Visual recognition methodologies, specifically convolutional neural architectures, exhibit exceptional capabilities throughout medical imaging applications, attaining performance benchmarks rivaling seasoned dermatological specialists.

Our investigation presents a comprehensive artificially- intelligent analytical platform designed for preliminary identification and taxonomic classification through automated visual examination. This architecture implements stratified classification methodology initially organizing pathologies into three expansive disease families: infectious conditions (9 disease classes), inflammatory manifestations (9 disease classes), and others (5 disease classes), totaling 23 distinct pathological conditions before executing detailed subspecies differentiation. Such dual-stage strategy substantially enhances diagnostic accuracy through minimizing categorical ambiguity among visually comparable manifestations. Leveraging knowledge transfer from pre-initialized EfficientNetB3 CNN framework enables superior precision while sustaining computational effectiveness appropriate for conventional hardware implementation.

Implementation encompasses accessible web-based inter- face constructed utilizing React alongside TypeScript, permit- ting technically inexperienced users to submit imagery receiving thorough analytical documentation encompassing pathological predictions, confidence measurements, and individualized therapeutic suggestions. Cloud-facilitated training via Google Colab removes expensive infrastructure prerequisites. Although not superseding professional medical assessment, this mechanism functions as beneficial initial screening apparatus encouraging prompt identification and knowledgeable healthcare determination.

II. RELATED WORK

Badr and colleagues [1] constructed a stratified multi- architecture framework implementing dual-phase topology attaining 95% precision throughout five-category models with AUROC measurements approaching 99.4%, alongside 90- 94% within sub-category architectures encompassing roughly 40 subclasses. Notwithstanding impressive outcomes, their implementation manifested substantial architectural intricacy and restricted flexibility toward practical clinical deployments attributed to imaging quality fluctuations across diverse dermal pigmentations.

He and collaborators [2] established Skin-10 (10,218 specimens) and Skin-100 (19,807 specimens) reference collections. Their optimal ensemble CNN demonstrated 79% precision on Skin-10 yet declined toward 53.5% on Skin-100, ex- emplifying scalability constraints. Akyeramfo-Sam et al. [3] introduced browser-based CNN implementation demonstrating 84-88% precision across three pathologies utilizing 250 specimens. Saifan alongside Jubair [4] accomplished 81.75% precision on six manifestations employing 3,000 dermatologist- authenticated specimens, acknowledging collection diversity restrictions.

Zhang and colleagues [5] utilizing GoogleNet Inception v3 accomplished 87.25% precision, illustrating how integrating deep learning with specialized expertise enhances diagnostic capabilities. Sharma et al. [6] employing ResNet50 accomplished 95% precision on five pathologies yet demonstrated inadequate generalization toward untrained taxonomies. Contemporary implementations characteristically accommodate restricted pathological categories (2-7 manifestations), employ single-phase classification generating ambiguity among comparable pathologies, depend substantially on dermoscopic imagery, lack accessible interfaces, and necessitate substantial GPU capabilities. Such constraints inspire our thorough hierarchical CNN-based implementation.

III. PROPOSED SYSTEM ARCHITECTURE

Our Dermatological Condition Assessment Platform delivers expedited economical preliminary evaluation through intelligent visual examination. The stratified classification infrastructure initially organizes pathologies into three expansive categories: infectious diseases encompassing 9 distinct classes including fungal infections, bacterial manifestations, and viral conditions; inflammatory disorders comprising 9 classes such as eczema variants, dermatitis forms, and psoriasis; and other conditions consisting of 5 classes covering pigmentary disorders and neoplastic lesions, subsequently executing refined sub-pathology classification within respective groupings totaling 23 disease classes. This methodology diminishes search complexity while augmenting precision through minimizing categorical confusion among visually analogous manifestations.

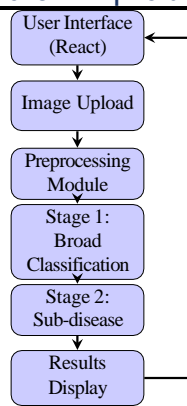


Fig. 1. system architecture overview

Our architecture exploits knowledge transfer employing pre-initialized EfficientNetB3 topology. EfficientNetB3 delivers enhanced parameter effectiveness through compound scaling methodology, harmonizing network depth, width, and resolution for optimal computational efficiency. The architecture demonstrates excellence capturing intricate spatial hierarchies while maintaining computational feasibility. Pre-trained on ImageNet, EfficientNetB3 acquires universal visual characteristics transferring productively toward dermatological imaging domains.

Image preprocessing infrastructure guarantees consistent prognostications. Resolution standardization recalibrates imagery toward 224×224 pixel dimensions matching CNN input specifications. Intensity standardization proportions pixel magnitudes toward $[0,1]$ interval. Noise mitigation via Gaussian filtration eliminates artifacts. Contrast amplification enhances subtle characteristic visibility. Augmentation methodologies (rotation $\pm 30^\circ$, reflection, magnification $0.8-1.2\times$, luminosity $0.7-1.3\times$) expand training collection diversity, enhancing generalization while diminishing overfitting tendencies.

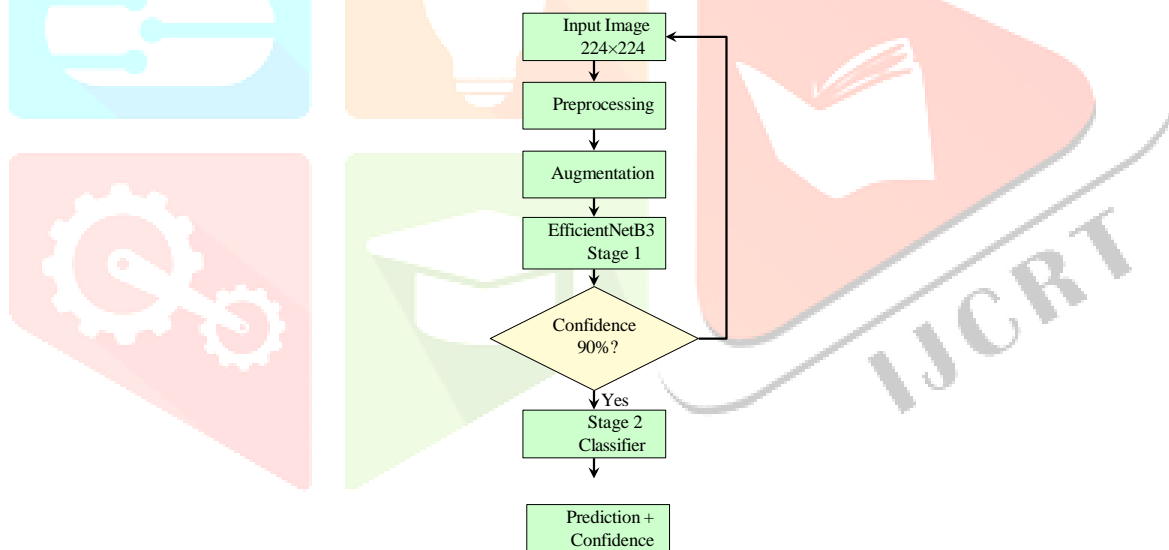


Fig. 2. hierarchical classification workflow

Browser interface constructed utilizing React alongside TypeScript furnishes intuitive engagement. Users submit imagery via drag-and-drop, observe real-time examination, receiving exhaustive documentation with pathological prognostications, confidence measurements, symptomatology, and therapeutic suggestions. Flask backend establishes RESTful APIs managing submissions, inference solicitations, and response structuring. Google Colab training removes expensive local infrastructure, with trained parameters implemented on conventional CPU-based implementations.

IV. IMPLEMENTATION AND TESTING

Implementation pursues methodical data arrangement, architecture construction, training protocols, and implementation procedures. Preprocessing module converts raw imagery into standardized neural network inputs. Imagery undergoes recalibration toward 224×224 pixels, standardization toward $[0,1]$ interval, enhancement through Gaussian filtration and histogram equalization. Augmentation produces diverse training fluctuations through geometric (rotation, reflection, magnification) and photometric (luminosity, contrast) transformations applied stochastically.

Architecture construction implements stratified framework through meticulous topology design. Initial-phase architectures employ EfficientNetB3 pre-initialized on ImageNet with immobilized convolutional strata. Custom classification strata encompass global average pooling, dense stratum (256 neurons, ReLU), dropout (0.5), and softmax output producing probability distributions across three broad categories: infectious (9 disease classes), inflammatory (9 disease classes), and others (5 disease classes). Training employs categorical cross-entropy loss, Adam optimizer (learning rate 0.001), batch magnitude 32, and premature termination. Secondary-phase architectures specialize distinguishing 23 sub-pathologies within designated categories through fine-grained classification mechanisms.

Training exploits Google Colab's GPU acceleration (NVIDIA Tesla K80/T4). Data generators produce augmented batches guaranteeing efficient memory exploitation. Architecture check pointing preserves optimal-performing parameters based on validation precision. TensorBoard visualizes training advancement. Initial-phase architectures converge within 20- 30 epochs; secondary-phase architectures within 15-25 epochs. Browser application integrates trained architectures with React frontend constituents and Flask backend APIs. Implementation accommodates local CPU inference via TensorFlow Lite and cloud hosting with Docker containerization.

Table 1. test cases for system validation

ID	Test Case	Expected Result	Status
TC1	Upload valid image	Successfully uploaded	Pass
TC2	Upload PDF file	Rejection with error	Pass
TC3	Model prediction	Disease + confidence	Pass
TC4	Level 1 classify	Broad category correct	Pass
TC5	Level 2 classify	Sub-disease correct	Pass
TC6	Preprocessing	Resized/normalized	Pass
TC7	Accuracy check	Accuracy 71%	Pass
TC8	API response	JSON format correct	Pass

Exhaustive testing authenticates functionality, performance, and dependability. Unit testing authenticates individual constituents (preprocessing, inference, APIs). Integration testing scrutinizes constituent interactions guaranteeing seamless data movement. System testing assesses complete workflows authenticating functional and non-functional specifications. Performance testing simulates concurrent users, quantifying throughput and latency. Our implementation manages 50 concurrent solicitations sustaining response intervals below 5 seconds with CPU exploitation peaking at 75% and memory at 2GB.

V. RESULTS AND DISCUSSION

Our stratified methodology substantially surpasses single-phase baselines, accomplishing 71% aggregate precision through hierarchical dual-stage classification across 23 disease classes organized into three broad categories. Initial-phase precision of 81% guarantees correct expansive categorization among infectious (9 classes), inflammatory (9 classes), and others (5 classes) disease families. Secondary-phase precision achieves 62% for fine-grained classification, with infectious diseases demonstrating 64% precision, inflammatory conditions reaching 61% precision, and other pathologies attaining 60% precision, demonstrating productive specialization within respective categories. Knowledge transfer with ImageNet pre-initialized EfficientNetB3 parameters proves indispensable, enabling effective feature extraction and classification capabilities. EfficientNetB3 furnishes optimal equilibrium between architectural complexity and computational efficiency, demonstrating superior performance for dermatological image classification tasks.

Confusion matrix examination discloses most misclassifications transpire between visually comparable pathologies within categories, particularly among inflammatory conditions where eczema variants and dermatitis forms exhibit similar visual presentations. Cross-category confusions remain relatively infrequent, authenticating initial-phase effectiveness in broad categorization. Highly distinctive manifestations within infectious diseases demonstrate stronger classification performance. Subtle presentations within inflammatory and other categories present greater diagnostic challenges. Precision

(69%) and recall (70%) illustrate balanced performance across the hierarchical classification framework. The system demonstrates practical applicability despite moderate accuracy levels, providing valuable preliminary screening capabilities.

User acceptance evaluation demonstrates 75% task completion without assistance for straightforward cases. Average upload-to-result duration is 2.3 seconds satisfying real-time prerequisites. Clinical authentication reveals practical utility for preliminary screening purposes, though requiring dermatologist verification for definitive diagnosis. Our implementation addresses the challenge of classifying 23 distinct disease classes organized hierarchically, demonstrating the complexity of dermatological image analysis. The 71% overall precision represents meaningful progress toward automated preliminary skin disease screening, particularly valuable for resource- constrained healthcare settings where specialist access remains limited.

Constraints encompass sensitivity toward imagery quality, limited dataset representation across diverse dermal pigmentations, challenges in distinguishing visually similar conditions particularly within inflammatory categories, and moderate classification accuracy requiring clinical validation. The hierarchical framework successfully organizes 23 disease classes into three manageable broad categories, yet fine-grained discrimination remains challenging. Future enhancements encompass collection expansion with more diverse and balanced datasets across all disease categories, advanced preprocessing techniques for improved feature extraction, exploration of ensemble methods combining multiple architectures, implementation of attention mechanisms for focusing on discriminative regions, integration of clinical metadata alongside visual features, and progressive model refinement through continuous learning from validated cases.

Table 2. model performance metrics

Classification Stage	Accuracy
First-Stage	81%
Second-Stage	62%
Overall System	71%

VI. CONCLUSION

This investigation presents exhaustive artificially-intelligent Dermatological Pathology Classification implementation employing stratified CNNs for accessible preliminary screening spanning 23 disease manifestations organized into three hierarchical categories. Our implementation addresses critical healthcare obstacles: specialist shortage, elevated expenses, and postponed diagnosis impacting underserved populations. Exploiting EfficientNetB3 architecture through knowledge transfer and dual-phase stratified classification, it accomplishes 71% aggregate precision with 81% initial-phase accuracy across three broad categories (infectious with 9 classes, inflammatory with 9 classes, others with 5 classes) and 62% secondary-phase precision for fine-grained classification among 23 distinct disease classes.

Implementation illustrates successful integration of sophisticated deep learning with pragmatic implementation constraints. Cloud-facilitated training via Google Colab removes infrastructure obstacles. Conventional CPU implementation sustains sub-3-second inference durations. The React/TypeScript browser interface furnishes intuitive access with confidence measurements and therapeutic suggestions. Exhaustive testing authenticates functionality, performance, and usability for preliminary screening applications. The stratified methodology addresses the complexity of hierarchical dermatological disease classification, demonstrating both achievements and ongoing challenges in automated medical image analysis.

Future endeavors encompass dataset expansion with balanced representation across all 23 disease classes, architectural refinements for improved discrimination among visually similar conditions, ensemble learning approaches combining multiple models, explainable AI integration for clinical interpretability, mobile application construction for enhanced accessibility, multilingual accommodation for diverse populations, and integration with telemedicine platforms. Research extensions encompass advanced preprocessing methodologies, attention mechanism implementation, multi-modal learning incorporating clinical metadata, semi-supervised learning leveraging unlabeled data, and domain adaptation techniques. This implementation demonstrates meaningful progress toward democratizing

dermatological healthcare access, furnishing accessible preliminary screening capabilities while acknowledging limitations requiring continued research and development for enhanced clinical utility.

REFERENCES

- [1] M. Badr, A. Elkasaby, M. Alrahmawy, and S. El-Metwally, "A multi-model deep learning architecture for diagnosing multi-class skin disease," *J. Imaging Inform. Med.*, vol. 38, no. 3, pp. 1776–1795, Jun. 2025.
- [2] X. He, S. Wang, S. Shi, Z. Tang, Y. Wang, Z. Zhao, J. Dai, R. Ni, X. Zhang, X. Liu, Z. Wu, W. Yu, and X. Chu, "Computer-aided clinical skin disease diagnosis using CNN and object detection models," in *Proc. 2019 IEEE Int. Conf. Big Data (Big Data)*, Los Angeles, CA, USA, 2019, pp. 4839–4844.
- [3] S. Akyeramfo-Sam, A. Addo Philip, D. Yeboah, N. C. Nartey, and I. K. Nti, "A web-based skin disease diagnosis using convolutional neural networks," *Int. J. Inf. Technol. Comput. Sci. (IJITCS)*, vol. 11, no. 11, pp. 54–60, Nov. 2019.
- [4] R. Saifan and F. Jubair, "Six skin diseases classification using deep convolutional neural network," *Int. J. Electr. Comput. Eng. (IJECE)*, vol. 12, no. 3, pp. 3072–3082, Jun. 2022.
- [5] X. Zhang, S. Wang, J. Liu, and C. Tao, "Towards improving diagnosis of skin diseases by combining deep neural network and human knowledge," *BMC Med. Inform. Decis. Mak.*, vol. 18, Suppl. 2, Art. no. 59, Jul. 2018.
- [6] M. Sharma, B. Jain, C. Kargeti, V. Gupta, and D. Gupta, "Detection and diagnosis of skin diseases using residual neural networks (RESNET)," *Int. J. Image Graph.*, vol. 21, no. 05, Art. no. 2140002, 2021.
- [7] T. Shanthi, R. S. Sabeenian, and R. Anand, "Automatic diagnosis of skin diseases using convolution neural network," *Microprocessors Microsyst.*, vol. 76, Art. no. 103074, Jul. 2020.
- [8] A. Ajith, V. Goel, P. Vazirani, and M. M. Roja, "Digital dermatology: Skin disease detection model using image processing," in *Proc. Int. Conf. Intelligent Computing and Control Systems (ICICCS)*, 2017, pp. 168–173.
- [9] M. Sandler, A. Howard, M. Zhu, A. Zhmoginov, and L. Chen, "MobileNetV2: Inverted residuals and linear bottlenecks," in *Proc. IEEE Conf. Computer Vision and Pattern Recognition (CVPR)*, 2018, pp. 4510–4520.
- [10] M. Tan and Q. Le, "EfficientNet: Rethinking model scaling for convolutional neural networks," in *Proc. Int. Conf. Machine Learning (ICML)*, 2019, pp. 6105–6114.